European Journal of Chemistry 14 (1) (2023) 80-89

European Journal of **Chem**istry

ATLANTA PUBLISHING HOUSE

View Journal Online
View Article Online

Fuel oil production from thermal decomposition of the model and waste polystyrene: Comparative kinetics and product distribution

Ghulam Ali [1,2,*], Jan Nisar [1] and Muhammad Arshad [2]

[1] *National Centre of Excellence in Physical Chemistry, University of Peshawar, 25120, Peshawar, Pakistan*
[2] *Bio/Chem Lab, Government Institute Kacha Mali Khel Dera Ismail Khan, Peshawar 25120, Pakistan*

* *Corresponding author at: National Centre of Excellence in Physical Chemistry, University of Peshawar, 25120, Peshawar, Pakistan.*
e-mail: ghulamali@uop.edu.pk (G. Ali).

RESEARCH ARTICLE

10.5155/eurjchem.14.1.80-89.2374

Received: 30 November 2022
Received in revised form: 04 January 2023
Accepted: 14 January 2023
Published online: 31 March 2023
Printed: 31 March 2023

KEYWORDS

Fuel oil
Kinetic models
Pyrolysis GC/MS
Products distribution
Arrhenius parameters
Thermokinetic analysis

ABSTRACT

The thermal degradation of model polystyrene (MPS) and waste polystyrene (WPS) was performed in a thermobalance system at four heating rates (β) *i.e.*, 5, 10, 15 and 20 °C/min, in an inert atmosphere. The apparent activation energy (E_a) and frequency factor (A) for the MPS and the WPS were calculated using Ozawa-Flynn-Wall (OFW), Kissinger-Akahira-Sunose (KAS), and Augis-Bennetis (AB) methods. It has been determined that E_a and A vary according to fraction conversion, heating rates, and applied models. The activation energy determined for MPS was found to be in the range of 91-106, 90-105, and 114-133 kJ/mol, while, for WPS, E_a was determined in the range of 82-160, 79-159 and 102-202 kJ/mol by applying OFW, KAS, and AB models, respectively. From the results obtained, it was concluded that the E_a determined by all of these methods increases with fraction conversion, indicating that the decomposition of polystyrene follows a complex mechanism of the solid-state reaction. Hence, the kinetic parameters, *i.e., E_a* and *A,* seem to play a key role in investigating the mechanism of solid-state reactions and will provide an opportunity to develop the mechanism of the industrial decomposition reactions. The results show that the MPS has a lower activation energy compared to WPS. This high E_a of WPS may be due to the additives used in the manufacturing of different polystyrene products. Pyrolysis GC/MS of WPS indicates that the main components of pyrolysis oil are 1-hydroxy-2-propanone, styrene, α-methyl styrene, toluene, and 1,2-dimethyl benzene. The presence of some oxygenated compounds in the fuel oil of WPS may be due to contamination or additives used during polystyrene processing, as the WPS samples were collected from a garbage dump near a local market. WPS can be utilized as fuel if the fuel oil collected from the pyrolysis of WPS is properly upgraded to make it equivalent to commercial fuel oil.

Cite this: *Eur. J. Chem.* **2023**, *14(1)*, 80-89 **Journal website**: www.eurjchem.com

1. Introduction

The majority of municipal and industrial plastic waste consists of waste polystyrene (WPS). Researchers have used various procedures to recycle WPS. Commonly used methods are physical recycling by mechanical and chemical mixing [1] and chemical reprocessing with polymer modification [2]. Thermal incineration [3] and thermal degradation [4] are the most common. The thermal decomposition of polystyrene (PS) is usually performed at elevated temperature with or without catalyst [5].

Thermal decomposition of WPS without catalyst at an appropriately high temperature results in comparable products of styrene monomers. Production of styrene and coke from WPS enhance the viscosity of the mixture and significantly decrease the heat transmission coefficient [6]. The pyrolysis process is the initial step of the thermochemical procedure that is carried out in the presence of a nitrogen gas. It is the process of thermal decom-position, based on a series of complicated mechanisms that are altered by various factors, *i.e.*, temperature, pressure, rate of heating, reaction time, and composition of the polymeric substance. Thermogravimetric analysis (TGA) is the basic method used for the kinetics of decomposition reactions of various substances. In the previous literature, many scientists used TGA and the resulting TGA data were interpreted to determine the kinetics of decomposition of various products, i.e., evaporation of natural fibers and other forms of biomass through a thermal degradation process [7].

Various methods are used to study the nonisothermal kinetic data obtained from TGA [8]. These techniques can be separated into two groups: (i) model-free (iso-conversional) and (ii) model-fitting methods. A greater number of analyses is required for the iso-conversional method. In the similar fraction conversion, the kinetic parameters are determined from several curves at different heating rate, β. Model fitting methods comprise by fitting various kinetic models to the data. The kinetic method that best fits the statistical data is selected for the kinetics study of the data.

In general, model-fitting methods were used for the kinetics of solid-state substances because of their ability to directly determine E_a and A from a single thermogravimetric (TG) data. Nevertheless, these procedures are affected by a number of

ISSN 2153-2249 (Print) / ISSN 2153-2257 (Online)
https://dx.doi.org/10.5155/eurjchem.14.1.80-89.2374

problems, one of them is their inability to determine the kinetic model [9], particularly for nonisothermal data; number of models can be found as statistically equal, however, the kinetic parameters i.e., E_a and A, can vary by an order of degree and therefore the selection of a proper kinetic method can be tricky. The use of model-fitting methods for nonisothermal figures gives greater values for kinetic parameters. The improvement of the model-free method starts with its straightforwardness and anticipation of errors associated with the selection of a kinetic reaction model [10]. These analyses permit the calculation of the E_a at a particular degree of conversion (α) for a free model. Using this method at different degrees of conversion, we get a series of E_a as a function of α. The fundamental statement is that the kinetic model (f(α)) is similar at a given degree of conversion (α) for a given reaction under various conditions [11]. The drawbacks of these analysis are a series of calculations at various heating rates, which should be done for the same weight of reaction samples and the same flow of nitrogen gas, and their variation can produce errors.

All model-free techniques are not isoconversional. The Kissinger technique is one of these exemptions, as it does not give E_a values at increasing degrees of conversion, but gives a constant E_a [12,13]. Peterson *et al.* investigated the thermo-oxidative and thermal degradation of PS [14]. The model-free iso-conversional procedures were used to determine the E_a. In nitrogen atmosphere, the calculated E_a for PS was observed at 200 kJ/mol and in the presence of air it was 125 kJ/mol. The thermal degradation of PS with hydrogen gas was carried out by Balakrishnan and Guria [15]. E_a and A were determined using the Arrhenius equation and were found to be 11.75 kcal/mol and 0.806 1/h, respectively. Aboulkas *et al.* determined the E_a of PS using the OFW method at different heating rates, i.e., 2, 10, 20, 50, and 100 K/min within a temperature range of 600 to 900 K [16]. The E_a calculated for PS was found to be 169 kJ/mol. Hydrated aluminum silicates were used for the catalytic decomposition of PS at 400 °C in a reactor. The order of the reaction determined was close to one, and the E_a calculated was found to be 350 kJ/mol. Mumbach *et al.* investigated thermal decomposition of plastic solid wastes. Various kinetic models were used to determine kinetic parameters [17]. The OFW, KAS, Starink and Vyazovkin models were used for the determination of the activation energy, and the resultant activation energy was observed to be 266.8, 268.3, 269.0 and 268.6 kJ/mol, respectively.

From the literature, it can be concluded that no research work is present on the comparison of the kinetics of MPS and WPS. This fact motivates us to investigate the comparative kinetics of degradation of model and waste PS. In this work, the pyrolysis of MPS and WPS will be carried out using TGA at four different heating rates. Thermal decomposition curves from TGA will be interpreted by applying OFW, KAS, and AB kinetic models, where A and E_a will be investigated from the intercept and slope of the kinetic plots. Thus, the kinetic data collected from the pyrolysis reaction will help in the utilization of MPS and WPS as energy sources. Moreover, MPS and WPS will be pyrolyzed into fuel oil in an indigenously manufactured furnace, and the pyrolysis oil collected will be characterized using various techniques.

2. Experimental

2.1. Material

The model polystyrene of laboratory reagent with a molecular weight of approximately 100000 was obtained from BDH Chemicals Ltd., Poole, England, whereas WPS was collected from a garbage dump near a local shopping market in Peshawar, Pakistan. The PS waste was shredded into pieces of almost 40/60 mesh by a shredder.

2.2. Thermogravimetric analysis

The thermogravimetric analysis (TGA) of MPS and WPS was performed on a PerkinElmer Diamond series TG/DTA instrument (USA). For TGA, approximately 7 mg of each TG sample was taken and heated from room temperature to the final 600 °C at heating rate of 5, 10, 15, and 20 °C/min. The sample temperature was measured and controlled by a thermocouple, attached directly with a pan very close to the PS sample. The TG data was used to calculate the Arrhenius parameters by using OFW, KAS, and AB methods.

2.3. Chemical kinetics

The kinetics of a reaction can be presented as follows:

$$\frac{d\alpha}{dt} = k(T)f(\alpha) \tag{1}$$

where dα/dt is the rate of conversion of the reactants and α is the conversion of the reactants. The conversion of reactants may be expressed in the form of Equation (2):

$$\alpha = \frac{m_i - m_a}{m_i - m_f} \tag{2}$$

where m_a is the actual mass, m_i is the initial mass, and m_f is the mass of the sample after pyrolysis. According to the Arrhenius Equation (3):

$$k = Ae^{{-Ea}/{RT}} \tag{3}$$

where A is the frequency factor, E_a is the activation energy, and R is the gas constant. By substituting the value of k from Equation (3) into Equation (1), Equation (4) was obtained.

$$\frac{d\alpha}{dt} = Af(\alpha)e^{{-Ea}/{RT}} \tag{4}$$

where $f(\alpha)$ is the conversion function. If the function $f(\alpha)$ is derivatized, then we have $f(\alpha)$ = -1. Several scientists restrict the function $f(\alpha)$ to Equation (5).

$$f(\alpha) = (1-\alpha)^n \tag{5}$$

By inserting Equation (5) into Equation (4), we obtain the reaction rate Equation (6):

$$\frac{d\alpha}{dt} = A(1-\alpha)^n e^{{-Ea}/{RT}} \tag{6}$$

For nonisothermal, we have

$$\frac{d\alpha}{dT} = \frac{d\alpha}{dt}\,\frac{dt}{dT} \tag{7}$$

where dt/dT is the opposite of the heating rate, dx/dt is the heating rate of isothermal processes, and dx/dT is the rate of nonisothermal processes. By combining Equation (6) into Equation (7), we obtain Equation (8):

$$\frac{d\alpha}{dT} = \frac{dt}{dT}\, A(1-\alpha)^n\, e^{{-Ea}/{RT}} \tag{8}$$

As dt/dT is the opposite of the heating rate, hence dt/dT = 1/β, by inserting the value of dt/dT into Equation (8), we obtained:

$$\frac{d\alpha}{dT} = \frac{A}{\beta}(1-\alpha)^n e^{{-Ea}/{RT}} \tag{9}$$

This expression shows the portion of the sample utilized in time t.

Table 1. Comparative kinetic parameters of the model and PS waste using the OFW method.

Alpha	OFW for model PS		OFW for waste PS	
	E_a (kJ/mol)	A (1/min)	E_a (kJ/mol)	A (1/min)
0.1	90.72	8.5×10^6	81.97	3.4×10^6
0.2	90.95	1.1×10^7	96.67	2.9×10^7
0.3	94.20	2.8×10^7	99.99	8.1×10^7
0.4	97.52	8.7×10^7	107.32	2.7×10^8
0.5	99.81	9.7×10^7	117.80	1.2×10^9
0.6	101.36	9.9×10^7	121.86	1.4×10^{10}
0.7	102.28	1.6×10^8	132.35	6.7×10^{10}
0.8	104.13	2.0×10^8	147.46	2.3×10^{11}
0.9	105.98	1.9×10^8	160.38	1.5×10^{13}

2.3.1. Ozawa-Flynn-Wall model

The OFW method [18] was used in the kinetic study by plotting the natural logarithm of the heating rates (ln β) versus 1/T. The final form of OFW expression can be presented as:

$$\ln(\beta_i) = \ln\left(\frac{A_\alpha Ea}{Rg(\alpha)}\right) - 5.331 - 1.052\frac{Ea}{RT} \tag{10}$$

where $g(\alpha)$ is an integral function that presents a constant conversion value [19].

2.3.2. Kissinger-Akahira-Sunose model

The KAS model [20,21] is a model-free method and can be plotted by the graph by plotting ln (β_i/T^2) versus *1*/T:

$$\ln\left[\frac{\beta_i}{T^2}\right] = \ln\left[\frac{A_\alpha R}{Eag(\alpha)}\right] - \frac{Ea}{RT} \tag{11}$$

2.3.3. Augis-Bennett's model

According to the AB model, the following Equation (12) can be used to determine the kinetic parameters [22].

$$\ln\left(\frac{\beta}{T_p - T_0}\right) = -\frac{Ea}{RT} + lnA \tag{12}$$

The plot of ln[$\beta/(T_p-T_o)$] versus 1/T presented straight-line curves, where E_a and *A* can be investigated from the linear plots.

2.4. GC/MS analysis

The fuel oil was collected from MPS and WPS decomposition within temperature range of 320-420 °C in the presence of inert gas. The pyrolysis product (bio-oil) collected was studied by Thermo Scientific DSQ II GC/MS system (USA) for product distribution.

3. Results and discussion

3.1. Ozawa-Flynn-Wall method for model and waste PS

The results obtained from TGA were evaluated to determine the kinetics parameters using model-free methods. The E_a and *A* at several degrees of conversion were calculated by applying the OFW, KAS, and AB equations, *viz*., Equations (10), (11), and (12), respectively. In the OFW method, ln β versus 1/T was extrapolated, which gives rise to a straight line as shown in Figure 1a and the resulting data are listed in Table 1. By applying the OFW equation, the activation energy, E_a, was determined in the range of 90.72 to 106.13 kJ/mol. The gradual increase in E_a with respect to fraction conversion prevails on the complex mechanism of PS decomposition. The preexponential factor, *A*, was also determined in each conversion fraction and was observed in the range of 8.5×10^6 to 2.0×10^8 min^{-1}. Peterson *et al.* determined the E_a in the presence and absence of oxygen [14]. Nitrogen was used as an inert gas. In the absence of air, the degradation of PS was performed and the calculated E_a was found to be about 200 kJ/mol. In thermo-oxidation, the E_a calculated for PS was lower than pyrolysis of PS in nitrogen medium and was found to be 125 kJ/mol. Pyrolysis experiments were performed by Westernhout [23] for the decomposition of PS in an inert atmosphere. In these experiments, isothermal TG analysis was carried out and E_a calculated for the degradation of PS was found to be 204 kJ/mol.

For waste PS, a series of linear fits plotted by applying the OFW equation and is given in Figure 1b. While the numerical results, that is, the kinetic parameters determined from the OFW plots, are listed in Table 1. The E_a increased from 83.0 to 164.4 kJ/mol with increasing fraction conversion. The *A* is determined at each fraction conversion, which also has a linear relation with fraction conversion. The increase in E_a with conversion is a sign of an indication that weaker bonds require less energy and are broken first, followed by the stronger linkage which requires a large amount of energy for breakage. Wu *et al.* obtained similar results on cracking of the municipal plastic waste mixture [24]. The apparent E_a of the decomposition reaction of the waste PS was determined to be 172 kJ/mol. Encinar and Gonzalez also studied the pyrolysis of PS; the apparent E_a calculated was found to be 137 kJ/mol [25].

3.2. KAS method for the model and waste PS

The KAS equation can be used to determine E_a and *A* by plotting ln (β/T^2) versus 1/T and the subsequent plots are presented in Figure 2a. The activation energy and preexponential factor values determined using the KAS method are listed in Table 2. At the start, the E_a was observed to be 89.6 kJ/mol, which increased to 105.7 kJ/mol at the final fraction conversion. Activation energy at 0.1, 0.2, and 0.7 fraction conversions is almost the same. The preexponential factor calculated from the KAS plots was found in the range of 1.7×10^7 to 4.6×10^8 min^{-1}. Senocak *et al.* investigated to determine the kinetic parameter of PS degradation in the presence of helium as an inert gas [26]. Friedman, Kissinger, OFW, and Coats-Redfern methods were applied for the determination of the E_a and F-factors. A kinetic study of PS was carried out using the OFW method, and E_a and *A* were determined and observed in the range of 179.7 to 200.36 kJ/mol and 7.2×10^{10} to 3.9×10^{12} min^{-1}, respectively.

Applying the KAS equation, ln(β/T^2) versus 1/T was plotted for WPS decomposition and the graphs obtained are shown in Figure 2b. For the determination of E_a and *A*, Equation (10) was used, and the resultant data is given in Table 2. The E_a values determined for the overall fraction conversion were observed in the range of 79.3 to 159.4 kJ/mol. Aguado *et al.* determined the E_a for the degradation of PS and found to be 137 kJ/mol [27]. Sorum *et al.* found parallel results for cracking of PS, the E_a of the degradation of PS was found to be 312 kJ/mol [28]. The initial E_a was low, which was due to the cleavage of some weak attractive forces and the elimination of volatile components from the PS. The strong bonds require greater energy to break, therefore a greater E_a is needed for the decomposition of these strong bonds [29,30].

Table 2. Comparative kinetics parameters of the model and waste PS using the KAS method.

Alpha	KAS for MPS		KAS for WPS	
	E_a (kJ/mol)	A (1/min)	E_a (kJ/mol)	A (1/min)
0.1	90.29	1.7×10^{7}	79.30	6.3×10^{6}
0.2	90.62	1.9×10^{7}	90.45	4.6×10^{7}
0.3	91.78	4.9×10^{7}	95.44	1.9×10^{8}
0.4	93.00	7.8×10^{8}	101.50	5.1×10^{8}
0.5	95.35	8.1×10^{8}	109.15	3.9×10^{9}
0.6	98.94	8.5×10^{7}	121.21	2.5×10^{10}
0.7	102.87	9.7×10^{7}	130.35	1.8×10^{11}
0.8	104.67	4.3×10^{8}	139.34	5.1×10^{11}
0.9	105.50	4.4×10^{8}	159.37	3.8×10^{13}

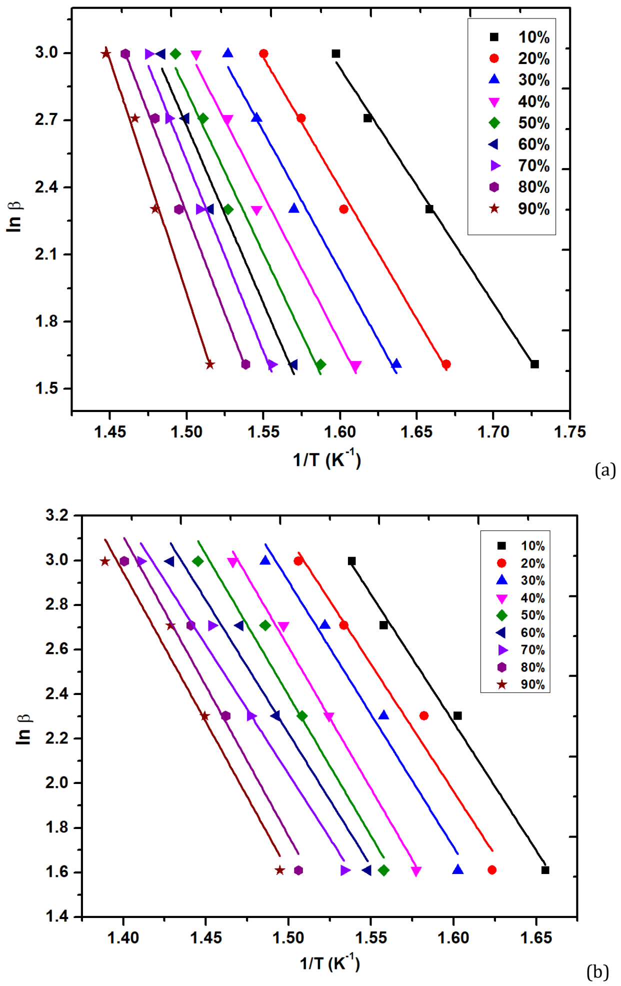

(a)

(b)

Figure 1. Kinetic analysis of (a) model PS and (b) waste PS at different fraction conversion by applying the OFW method.

3.3. AB method for the model and waste PS

The Augis-Bennetis equation was used to calculate the E_a and F-factors for MPS under the same conditions. E_a and A determined using the AB method are shown in Figure 3a and the resulting data listed in Table 3 and observed within the range of 114.06 to 134.27 kJ/mol and 1.0×10^{8} to 2.3×10^{9} min^{-1}, respectively. Blanco *et al.* investigated thermal and thermo-oxidative decomposition of polyethylene (PE), PS, poly(methyl methacrylate) (PMMA), and polycarbonate (PC) in a TG analyzer. The experiments were carried out at various temperatures [31]. The apparent E_a determined using the Kissinger method for PE, PS PMMA and PC was found to be 204, 149, 199 and 85 kJ/mol, respectively. Marcilla and Beltran studied the nonisothermal TGA of PS in a nitrogen atmosphere and found its E_a within the range of 203 to 276 kJ/mol [32].

For WPS, the AB method was used in which ln (β/T-T$_o$) was plotted against 1/T and the corresponding plots are shown in Figure 3b. The E_a and A of WPS determined are given in Table 3. The E_a starts from 102.21 kJ/mol and reaches 202.76 kJ/mol at maximum fraction conversion. At the beginning, the lower E_a is due to the decomposition of weak linkage, and the higher E_a may be attributed to the strong bonds. Balakrishnan and Guria determined E_a and A at low temperature [15]. The E_a and A were calculated using the Arrhenius equation and found to be 49.11 kJ/mol and 2.8×10^{7} sec^{-1}, respectively. Previously, researchers presumed that Arrhenius parameters *viz.* E_a and A remain constant throughout the reaction, but now it has been concluded that in solid state reactions, E_a and A vary with fraction conversion [33-34].

Table 3. Comparative kinetic parameters of the model and waste PS using the AB method

Alpha	AB for model PS		AB for waste PS	
	E_a (kJ/mol)	A (1/min)	E_a (kJ/mol)	A (1/min)
0.1	114.31	4.6×10^{8}	102.21	1.17×10^{8}
0.2	114.76	4.9×10^{8}	113.93	5.2×10^{8}
0.3	119.22	5.1×10^{8}	121.49	1.4×10^{9}
0.4	121.62	5.6×10^{9}	128.80	4.1×10^{9}
0.5	123.04	6.1×10^{9}	140.85	2.8×10^{10}
0.6	126.97	6.6×10^{8}	154.64	2.8×10^{11}
0.7	129.23	6.9×10^{8}	166.36	1.9×10^{12}
0.8	131.27	9.3×10^{8}	174.51	6.4×10^{12}
0.9	133.85	1.8×10^{9}	202.76	7.6×10^{14}

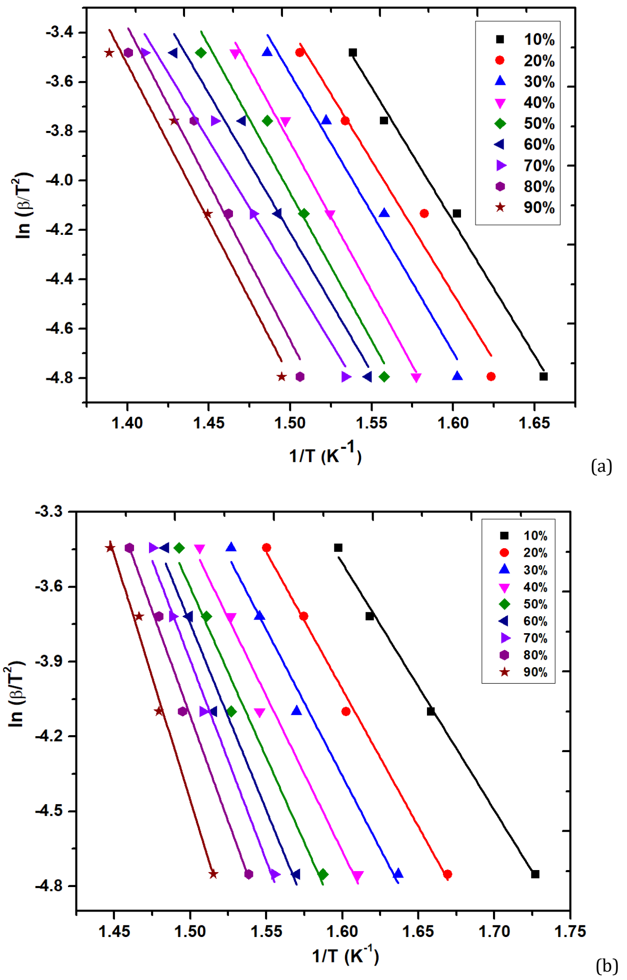

(a)

(b)

Figure 2. KAS plots for (a) model PS and (b) waste PS at different fraction conversion.

3.4. Comparison of kinetic models

The activation energy determined by different models for MPS was compared and the resultant graph is shown in the Figure 4a. The E_a manipulated using the OFW and KAS methods is in good agreement, whereas that of determined by the AB method is higher. The E_a determined for WPS by OFW, KAS, and AB methods is given in Figure 4b. The figure indicates the dependence of E_a on the different fraction conversion and additives, used in the PS products. Activation energies determined by OFW and KAS methods are almost the same, whereas E_a determined by the AB method is much higher. Comparison of Figures 4a and 4b indicates that the activation energies of WPS are higher than those of MPS. This higher E_a may be attributed to the additives used in the manufacture of PS products. The E_a determined for MPS and WPS was compared with the literature as given in Table 4. The table indicates that the E_a and A determined thermal decomposition of MPS and WPS is in good agreement with the reported values. However, some differences in E_a and A were observed, which may be due to the variation in sample size for each experiment, inconsistency in the flow of the inert gas, or due to the selection of the suitable kinetic model for the determination of kinetic parameters. However, the kinetic parameters, *viz.*, E_a and A, determined in our study may be supposed to be more reliable and consistent with each other with minimal exception.

3.5. Pyrolysis GC/MS

3.5.1. GC-MS of the fuel oil of model polystyrene

Pyrolysis products, *i.e.*, liquid oil collected in the reaction vessel, were analyzed by GC/MS and the subsequent chromatogram is shown in Figure 5. Figure 5 indicates that the pyrolysis oil obtained from MPS consists of 14 different components.

Table 4. Kinetic parameters (E_a and A) reported in the literature for the pyrolysis of PS

Temperature (°C)	E_a (kJ/mol)	A (1/min)	Methods	References
400-450	219	1.3×10^{14}	1st order kinetic	[23]
Room temp-600	139	$5..0\times10^{9}$	CR	[35]
Room temp-600	130	2.3×10^{10}	OFW	[35]
300-500	207	6.0×10^{4}	FM	[36]
200-260	149	8.8×10^{8}	Kissinger	[31]
50-600	200	3.9×10^{12}	OFW	[26]
40-800	242	2.65×10^{18}	FM	[36]
40-800	236	1.9×10^{17}	KAS	[36]
40-800	250	1.9×10^{13}	CR	[36]
0-1000	213	6.9×10^{13}	KAS	[37]
0-1000	214	6.9×10^{13}	OFW	[37]
0-1000	222	6.9×10^{13}	FM	[37]
Room temp-600	169	1.2×10^{13}	OFW	[12]
Room temp-600	163	3.4×10^{13}	KAS	[12]
Room temp-600	173	5.3×10^{13}	FM	[12]
Room temp-600	202	7.6×10^{14}	AB	[12]
Room temp-600	166	4.8×10^{11}	K	[12]
Room temp-600	82-160	3.4×10^{6}-1.5×10^{13}	OFW waste PS	Present work
Room temp-600	90-105	1.7×10^{7}-4.4×10^{8}	KAS model PS	Present work
Room temp-600	79-159	6.3×10^{6}-3.8×10^{13}	KAS waste PS	Present work
Room temp-600	114-134	4.6×10^{8}-1.8×10^{9}	AB model PS	Present work
Room temp-600	102-202	1.1×10^{8}-7.6×10^{14}	AB waste PS	Present work

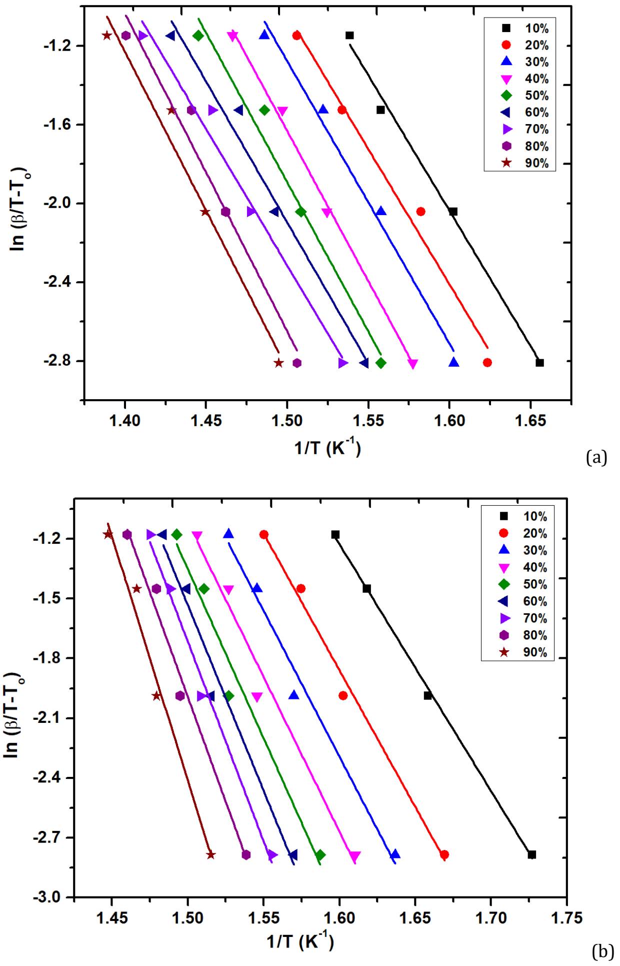

Figure 3. Augis and Bennetis plots at varying degrees of conversion for (a) model PS and (b) waste PS.

The details of each component with %area, %height and their chemical formula are given in Table 5. The table indicates that the liquid part of the MPS mainly contains benzene, 4-methyl-2-hexene, ethyl benzene, 2-hexene-3,5-dimethyl, α-methyl styrene and benzene-(1-methylethenyl) with a retention time of 7.42, 10.38, 10.85, 11.01 and 11.11 min and with %area of 5.33, 9.53, 9.47, 15.59 and 9.43%, respectively. Aljabri *et al.* studied the cracking of waste PS under mild conditions [38]. Liquid oil collected from the pyrolyzer was analyzed by GC/MS. The results indicate that the main components in the pyrolysis oil were ethyl benzene, α-methyl styrene and α-phenethyl styrene, which are in accordance with our data. Undri *et al.* investigated the pyrolysis products of WPS by GC/MS. The GC/MS plots of the WPS indicate that the main components in the liquid fraction were α-methylstyrene, benzene, styrene, and ethylbenzene [39].

Table 5. Products distribution in fuel oil obtained from the pyrolysis of waste PS

No	Retention time (min)	Products	Formula	Molecular weight (g)	% Area	% Height
1	5.67	Benzene	C_6H_6	78	11.23	12.11
2	5.89	2-methyl-3-pentene	C_6H_{12}	84	2.07	1.43
3	7.01	Toluene	C_7H_8	92	14.06	16.24
4	7.42	4-Methyl-2-hexene	C_7H_{11}	98	5.33	5.14
5	10.38	Ethyl benzene	C_8H_8	104	9.53	8.73
6	10.63	Chloroform	$CHCl_3$	118	2.91	1.64
7	10.85	2-Hexene3,5-dimethyl	C_8H_{16}	112	9.47	10.57
8	11.01	α-Methyl styrene	C_9H_{10}	118	15.59	16.23
9	11.11	Benzene-(1-methylethenyl)	$C_{10}H_{12}$	132	9.43	10.24
10	12.81	Tetra methyl benzene	$C_{10}H_{14}$	134	2.43	1.78
11	13.74	Naphthalene, 2-ethnyl-	$C_{12}H_{10}$	154	4.74	4.67
12	13.92	Propane, 1,3-biphenyl	$C_{15}H_{16}$	196	4.77	4.79
13	14.11	2-Phenylnaphthalene	$C_{16}H_{12}$	204	3.72	1.82
14	14.35	α-Phenethyl styrene	$C_{16}H_{16}$	208	4.72	4.61

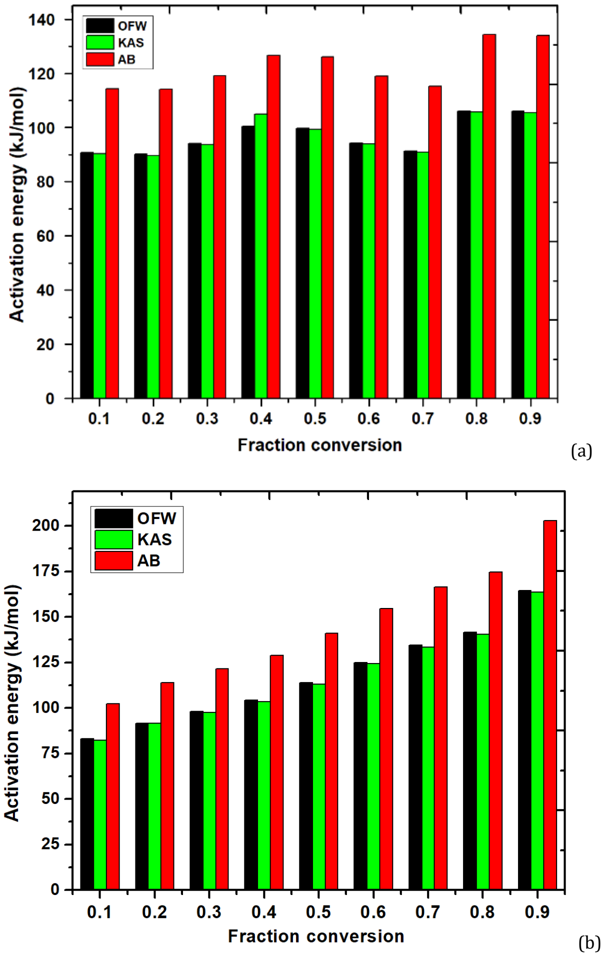

(a)

(b)

Figure 4. Comparative analysis of the activation energy of thermal decomposition of (a) model PS and (b) waste PS.

Ma *et al.* studied the thermal pyrolysis of PS [40]. Pyrolysis experiments were performed, and the fuel oil collected was examined by GC/MS. The main components observed in the GC/MS chromatogram were styrene, α-methyl styrene, and ethylbenzene.

3.5.2. Gas chromatography mass spectrometry of waste polystyrene

The pyrolysis of the WPS was carried out in a pyrolyzer at different temperatures of 320, 330, 340, 350, 360, 370, 380, 390, 400, 410 and 420 °C. The collected pyrolysis products were examined by GC/MS as shown in Figure 6, while the distribution of the resulting products is shown in Table 6. The results show that the main components of pyrolysis oil for waste polystyrene are 1-hydroxy-2-propanone with retention time of 1.70 min, styrene with retention time of 4.47 min, α-methyl styrene with retention time of 5.89 min and toluene with retention time of 1.36 min. The results indicate that the main hydrocarbons such as α-methyl styrene, toluene, and 1,2-dimethyl benzene are fuel-range hydrocarbons. The presence of oxygenated compounds in the fuel oil may be due to contamination or additives used during the processing of PS, since the waste PS samples were collected from a dumpsite. Waste PS can be utilized as fuel if the pyrolysis oil collected from the pyrolysis of waste PS is properly upgraded to make it equivalent to commercial fuel oil.

Ali *et al.* conducted pyrolysis of WPS in the presence of clay within a temperature of 340 to 420 °C in an inert atmosphere [5].

Table 6. Product distribution in fuel oil obtained from the pyrolysis of waste PS

No	Retention time (min)	Products	Formula	Molecular weight (g)	% Area	% Height
1	0.83	Ethyl alcohol	C_2H_6O	46	1.53	2.71
2	0.86	2-Propanone	C_3H_6O	58	3.76	9.11
3	0.97	Propanoic acid	$C_3H_6O_2$	74	1.36	1.81
4	1.36	Toluene/Methyl benzene	C_7H_8	92	4.01	11.82
5	1.41	Iso-propyl benzene	C_9H_{12}	120	1.86	3.34
6	1.70	1-Hydroxy-2-propanone	$C_3H_6O_2$	74	31.11	21.22
7	2.72	Trans-2-hexene	C_6H_{12}	84	1.77	3.45
8	3.93	1,2-Dimethyl benzene	C_8H_{10}	106	2.11	3.90
9	4.47	Styrene/Ethyl benzene	C_8H_8	104	34.55	16.92
10	5.89	Iso-propenyl benzene	C_9H_{10}	118	6.03	9.71
11	10.85	3,5-Dimethyl-1-hexyn-3-ol	$C_8H_{14}O$	126	2.71	3.41
12	11.09	Diphenyl methane	$C_{13}H_{26}$	168	1.34	2.32
13	12.81	2-Isopropyl-5-methyl-1-heptanol	$C_{11}H_{24}O$	172	2.57	3.76
14	13.86	Cycle-pentane-1, 2-dibutyl	$C_{11}H_{24}O$	172	2.63	4.01
15	13.97	1,3-Diphenyl propane	$C_{15}H_{16}$	196	1.37	2.51

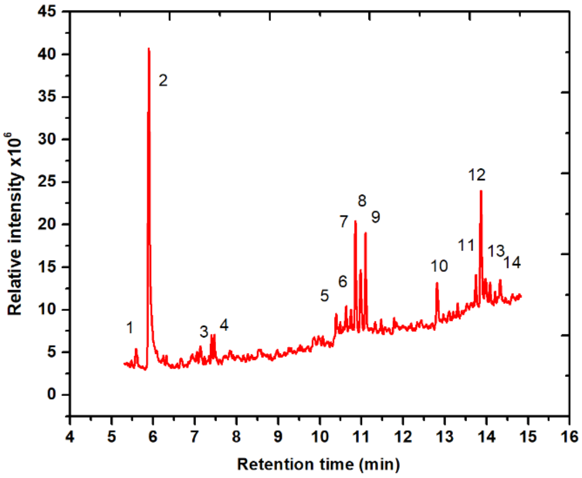

Figure 5. GC/MS chromatogram of fuel oil collected from the pyrolysis of the model PS.

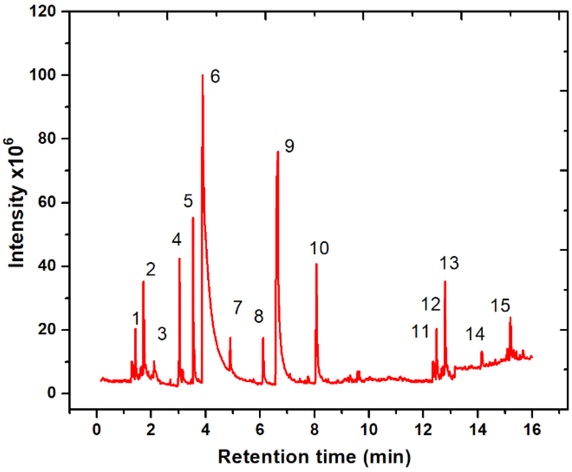

Figure 6. GC/MS chromatogram of fuel oil obtained from the pyrolysis of waste PS.

Pyrolysis products produced were collected and analyzed by GC/MS. The fuel oil consisted mainly of alkanes, alkenes, and aromatics. The results indicate that the two main peaks with chromatogram peak heights of 17.9 and 11.31% at retention times of 7.19 and 8.18 min corresponded to α-methyl styrene and 2-phenyl ethanol, respectively. The second group of peaks consists of peak heights of 6.11, 5.67, 9.73, and 6.31% and was observed at retention time of 3.50, 6.91, 14.14 and 11.16 min assigned to 2-propanone, styrene, 1,3-diphenyl propane and 2,4-diethyl-1-heptanol, respectively. Peaks that were studied at retention time of 9.53, 2.78, 5.35; 13.50, 15.91, 21.51, and 16.55 min correspond to 2-isopropyl-5-methyl-1-heptanol, 1-propene-2-methyl, *o*-xylene, diphenyl methane, 1,2-diphenyl cyclopropane, 1-dodecanol-3,7,11-trimethyl and 2,4-diphenyl-1-butene, respectively.

4. Conclusions

The thermal degradation of PS was found to be a very useful technique for utilizing plastic waste. Pyrolysis GC/MS of fuel oil of the MPS indicates mainly contains benzene, 4-methyl-2-hexene, ethyl benzene, 2-hexene-3,5-dimethyl, α-methyl styrene and benzene-(1-methylethenyl) with a retention time of 7.42, 10.38, 10.85, 11.01 and 11.11 min and with %area of 5.33, 9.53, 9.47, 15.59 and 9.43%, respectively. The WPS pyrolysis oil consists mainly of 1-hydroxy-2-propanone, styrene, α-methyl styrene, toluene, α-methyl styrene, toluene and 1,2-dimethyl benzene. The presence of microoxygenated compounds in the fuel oil of waste PS may be due to contamination or due to additives used during the processing of PS, as the WPS samples were collected from a dumpsite. Waste PS can be utilized as fuel if the fuel oil collected from the pyrolysis of WPS is properly upgraded to make it equivalent to commercial fuel oil.

The thermal degradation kinetics was performed by TGA at a temperature of 30-600 °C. OFW, KAS, and AB methods were applied to the TG data to determine the Arrhenius parameters (E_a, A). The activation energy investigated for MPS was found to be ranging 91-106, 90-105, and 114-133 kJ/mol using OFW, KAS, and AB models, respectively. Whereas E_a for WPS using OFW, KAS, and AB methods was observed within the range of 82-160, 79-159, and 102-202 kJ/mol, respectively. It was found that the E_a determined by all three methods increases with fraction conversion, indicating the complex mechanism of solid-state reaction. The results prevail that the MPS has lower E_a compared to the WPS. The higher energy of waste polystyrene may be due to the additives used in the manufacturing of different polystyrene products. The kinetic parameters are considered to be very useful in determining the reaction mechanism of solid-state reactions in an industrial system.

Acknowledgement

The support extended by the Higher Education Commission of Pakistan is greatly appreciated.

Disclosure statement

Conflict of interest: The authors declare that they have no conflict of interest.
Ethical approval: All ethical guidelines have been adhered.

CRediT authorship contribution statement

Conceptualization: Ghulam Ali; Methodology: Ghulam Ali; Software: Ghulam Ali; Validation: Ghulam Ali, Muhammad Arshad; Formal Analysis: Muhammad Arshad; Investigation: Ghulam Ali; Resources: Ghulam Ali; Data Curation: Ghulam Ali; Writing - Original Draft: Ghulam Ali; Writing - Review and Editing: Ghulam Ali; Visualization: Muhammad Arshad; Funding acquisition: Jan Nisar; Supervision: Jan Nisar; Project Administration: Jan Nisar.

ORCID and Email

Ghulam Ali
ghulamai@uop.edu.pk
https://orcid.org/0000-0002-7995-3925
Jan Nisar
jan_nisar@uop.edu.pk
https://orcid.org/0000-0002-6072-6255
Muhammad Arshad
ghulamali437@gmail.com
https://orcid.org/0000-0002-8896-9814

References

[1]. Ali, G.; Nisar, J. Kinetics and thermodynamics of the pyrolysis of waste polystyrene over natural clay. *Adv. Environ. Eng. Res.* **2022**, *03*, 1–40.

[2]. Karagöz, S.; Karayildirim, T.; Uçar, S.; Yuksel, M.; Yanik, J. Liquefaction of municipal waste plastics in VGO over acidic and non-acidic catalysts☆. *Fuel (Lond.)* **2003**, *82*, 415–423.

[3]. Ohta, M.; Oshima, S.; Osawa, N.; Iwasa, T.; Nakamura, T. Formation of PCDDs and PCDFs during the combustion of polyvinylidene chloride and other polymers in the presence of HCl. *Chemosphere* **2004**, *54*, 1521–1531.

[4]. Woo, O. S.; Ayala, N.; Broadbelt, L. J. Mechanistic interpretation of base-catalyzed depolymerization of polystyrene. *Catal. Today* **2000**, *55*, 161–171.

[5]. Ali, G.; Nisar, J.; Shah, A.; Farooqi, Z. H.; Iqbal, M.; Shah, M. R.; Ahmad, H. B. Production of liquid fuel from polystyrene waste: Process optimization and characterization of pyrolyzates. *Combust. Sci. Technol.* **2021**, 1–14.

[6]. Ukei, H.; Hirose, T.; Horikawa, S.; Takai, Y.; Taka, M.; Azuma, N.; Ueno, A. Catalytic degradation of polystyrene into styrene and a design of recyclable polystyrene with dispersed catalysts. *Catal. Today* **2000**, *62*, 67–75.

[7]. Nisar, J.; Nasir, U.; Ali, G.; Shah, A.; Farooqi, Z. H.; Iqbal, M.; Shah, M. R. Kinetics of pyrolysis of sugarcane bagasse: effect of catalyst on activation energy and yield of pyrolysis products. *Cellulose* **2021**, *28*, 7593–7607.

[8]. Šimon, P. Isoconversional methods. *J. Therm. Anal. Calorim.* **2004**, *76*, 123–132.

[9]. Khawam, A.; Flanagan, D. R. Complementary use of model-free and modelistic methods in the analysis of solid-state kinetics. *J. Phys. Chem. B* **2005**, *109*, 10073–10080.

[10]. Opfermann, J. R.; Kaisersberger, E.; Flammersheim, H. J. Model-free analysis of thermoanalytical data-advantages and limitations. *Thermochim. Acta* **2002**, *391*, 119–127.

[11]. Zhou, D.; Schmitt, E. A.; Zhang, G. G.; Law, D.; Vyazovkin, S.; Wight, C. A.; Grant, D. J. W. Crystallization kinetics of amorphous nifedipine studied by model-fitting and model-free approaches. *J. Pharm. Sci.* **2003**, *92*, 1779–1792.

[12]. Nisar, J.; Ali, G.; Shah, A.; Iqbal, M.; Khan, R. A.; Sirajuddin; Anwar, F.; Ullah, R.; Akhter, M. S. Fuel production from waste polystyrene via pyrolysis: Kinetics and products distribution. *Waste Manag.* **2019**, *88*, 236–247.

[13]. Nisar, J.; Ali, G.; Shah, A.; Shah, M. R.; Iqbal, M.; Ashiq, M. N.; Bhatti, H. N. Pyrolysis of expanded waste polystyrene: Influence of nickel-doped copper oxide on kinetics, thermodynamics, and product distribution. *Energy Fuels* **2019**, *33*, 12666–12678.

[14]. Peterson, J. D.; Vyazovkin, S.; Wight, C. A. Kinetics of the Thermal and Thermo-Oxidative Degradation of Polystyrene, Polyethylene and Poly(propylene). *Macromolecular Chemistry and Physics* **2001**, *202*, 775–784.

[15]. Balakrishnan, R. K.; Guria, C. Thermal degradation of polystyrene in the presence of hydrogen by catalyst in solution. *Polym. Degrad. Stab.* **2007**, *92*, 1583–1591.

[16]. Aboulkas, A.; El harfi, K.; El Bouadili, A. Thermal degradation behaviors of polyethylene and polypropylene. Part I: Pyrolysis kinetics and mechanisms. *Energy Convers. Manag.* **2010**, *51*, 1363–1369.

[17]. Mumbach, G. D.; Alves, J. L. F.; Da Silva, J. C. G.; De Sena, R. F.; Marangoni, C.; Machado, R. A. F.; Bolzan, A. Thermal investigation of plastic solid waste pyrolysis via the deconvolution technique using the asymmetric double sigmoidal function: Determination of the kinetic triplet, thermodynamic parameters, thermal lifetime and pyrolytic oil composition for clean energy recovery. *Energy Convers. Manag.* **2019**, *200*, 112031.

[18]. Flynn, J. H.; Wall, L. A. A quick, direct method for the determination of activation energy from thermogravimetric data. *J. Polym. Sci. B* **1966**, *4*, 323–328.

[19]. Ali, G.; Nisar, J.; Iqbal, M.; Shah, A.; Abbas, M.; Shah, M. R.; Rashid, U.; Bhatti, I. A.; Khan, R. A.; Shah, F. Thermo-catalytic decomposition of polystyrene waste: Comparative analysis using different kinetic models. *Waste Manag. Res.* **2020**, *38*, 202–212.

[20]. Kissinger, H. E. Variation of peak temperature with heating rate in differential thermal analysis. *J. Res. Natl. Bur. Stand. (1934)* **1956**, *57*, 217.

[21]. Nisar, J.; Khan, M. A.; Ali, G.; Iqbal, M.; Din, M. I.; Hussain, Z.; Bhatti, I. A.; Al-Kadhi, N. S.; Alamro, F. S. Polypropylene pyrolysis kinetics under isothermal and non-isothermal conditions: a comparative analysis. *Z. Phys. Chem. (N F)* **2022**, *236*, 1163–1172.

[22]. Chrissafis, K. Kinetics of thermal degradation of polymers: Complementary use of isoconversional and model-fitting methods. *J. Therm. Anal. Calorim.* **2009**, *95*, 273–283.

[23]. Westerhout, R. W. J.; Waanders, J.; Kuipers, J. A. M.; van Swaaij, W. P. M. Kinetics of the low-temperature pyrolysis of polyethene, polypropene, and polystyrene modeling, experimental determination, and comparison with literature models and data. *Ind. Eng. Chem. Res.* **1997**, *36*, 1955–1964.

[24]. Wu, C.-H.; Chang, C.-Y.; Hor, J.-L.; Shih, S.-M.; Chen, L.-W.; Chang, F.-W. On the thermal treatment of plastic mixtures of MSW: Pyrolysis kinetics. *Waste Manag.* **1993**, *13*, 221–235.

[25]. Encinar, J. M.; González, J. F. Pyrolysis of synthetic polymers and plastic wastes. Kinetic study. *Fuel Process. Technol.* **2008**, *89*, 678–686.

[26]. Şenocak, A.; Alkan, C.; Karadağ, A. Thermal decomposition and a kinetic study of poly(para-substituted styrene)s. *Am. J. Analyt. Chem.* **2016**, *07*, 246–253.

[27]. Aguado, R. Kinetics of polystyrene pyrolysis in a conical spouted bed reactor. *Chem. Eng. J.* **2003**, *92*, 91–99.

[28]. Sørum, L.; Grønli, M. G.; Hustad, J. E. Pyrolysis characteristics and kinetics of municipal solid wastes. *Fuel (Lond.)* **2001**, *80*, 1217–1227.

[29]. Heydari, M.; Rahman, M.; Gupta, R. Kinetic study and thermal decomposition behavior of lignite coal. *Int. J. Chem. Eng.* **2015**, *2015*, 1–9.

[30]. Nisar, J.; Ali, G.; Shah, A.; Farooqi, Z. H.; Khan, R. A.; Iqbal, M.; Gul, M. Pyrolysis of waste tire rubber: a comparative kinetic study using different models. *Energy Sources Recovery Util. Environ. Eff.* **2020**, 1–11.

[31]. Blanco, I.; Abate, L.; Antonelli, M. L. The regression of isothermal thermogravimetric data to evaluate degradation Ea values of polymers: A comparison with literature methods and an evaluation of lifetime prediction reliability. Polym. Degrad. Stab. 2011, 96, 1947–1954.

[32]. Marcilla, A.; Beltrán, M. Kinetic study of the thermal decomposition of polystyrene and polyethylene-vinyl acetate graft copolymers by thermogravimetric analysis. *Polym. Degrad. Stab.* **1995**, *50*, 117–124.

[33]. Vyazovkin, S. Evaluation of activation energy of thermally stimulated solid-state reactions under arbitrary variation of temperature. *J. Comput. Chem.* **1997**, *18*, 393–402.

[34]. Vyazovkin, S. Kinetic concepts of thermally stimulated reactions in solids: A view from a historical perspective. *Int. Rev. Phys. Chem.* **2000**, *19*, 45–60.

[35]. Nisar, J.; Ali, G.; Shah, A.; Farooqi, Z. H.; Iqbal, M.; Khan, S.; Sherazi, S. T. H.; Sirajuddin Production of fuel oil and combustible gases from pyrolysis of polystyrene waste: Kinetics and thermodynamics interpretation. *Environ. Technol. Innov.* **2021**, *24*, 101996.

[36]. Cheng, J.; Pan, Y.; Yao, J.; Wang, X.; Pan, F.; Jiang, J. Mechanisms and kinetics studies on the thermal decomposition of micron Poly (methyl methacrylate) and polystyrene. *J. Loss Prev. Process Ind.* **2016**, *40*, 139–146.

[37]. Özsin, G.; Pütün, A. E. Insights into pyrolysis and co-pyrolysis of biomass and polystyrene: Thermochemical behaviors, kinetics and evolved gas analysis. *Energy Convers. Manag.* **2017**, *149*, 675–685.

[38]. Aljabri, N. M.; Lai, Z.; Hadjichristidis, N.; Huang, K.-W. Renewable aromatics from the degradation of polystyrene under mild conditions. *J. Saudi Chem. Soc.* **2017**, *21*, 983–989.

[39]. Undri, A.; Frediani, M.; Rosi, L.; Frediani, P. Reverse polymerization of waste polystyrene through microwave assisted pyrolysis. *J. Anal. Appl. Pyrolysis* **2014**, *105*, 35–42.

[40]. Ma, C.; Yu, J.; Wang, B.; Song, Z.; Xiang, J.; Hu, S.; Su, S.; Sun, L. Catalytic pyrolysis of flame retarded high impact polystyrene over various solid acid catalysts. *Fuel Process. Technol.* **2017**, *155*, 32–41.